



OPEN Versatile and portable Cas12a-mediated detection of antibiotic resistance markers

Maryhory Vargas-Reyes^{1,2}, Roberto Alcántara^{1,3}✉, Soraya Alfonsi³, Katherin Peñaranda^{1,3}, Dezemona Petrelli³, Roberto Spurio³, Monica J. Pajuelo² & Pohl Milon¹✉

Antibiotic-resistant bacteria are spreading in clinical, industrial, and environmental ecosystems. The spreading dynamics to and from the environment are unknown, largely due to the lack of appropriate (robust, fast, low-cost) analytical assays. In this study, we developed C12a, a versatile molecular toolbox to detect genetic markers of antibiotic resistance using CRISPR/Cas12a. Biochemical characterization show that the C12a toolbox can detect less than 100 attoMolar of pure DNA fragments from the *bla*CTX-M15 and *flo*R genes, conferring resistance to β -lactams and amphenicols, respectively important for human and veterinary uses. In microbiological assays, C12a detected less than 10² CFU/mL and high concordance was observed if compared to antibiotic susceptibility tests, PCR, or to whole genome sequencing. Additionally, C12a confirmed a high prevalence of the integrase/integron system in *E. coli* isolates containing multiple antibiotic resistance genes (ARGs). The C12a toolbox shows equivalent detection performance in diverse laboratory settings, results readout (Fluorescence vs. FLA) or input sample. Altogether, this work presents a comprehensive proof-of-concept, development description, and biochemical characterization of a collection of molecular tools to detect antibiotic resistance markers in a one health setup.

Keywords Antibiotic resistance gene, Cas12a, *bla*CTX, *flo*R, Integrase

The discovery of antibiotics allowed control of bacterial infections, improving surgical outcomes, treating infectious diseases, and boosting farm productivity, ultimately contributing to increased life expectancy¹. However, the antimicrobial resistance (AMR) threat accelerated due to the combination of multiple interconnected factors, including antibiotic overuse^{2,3}, complex ecological factors^{4,5}, ineffective waste management and mechanisms of spread by horizontal gene transfer⁶. Effective surveillance strategies are lacking due to insufficient capacities for sensitive, timely, cost-effective, and accurate monitoring^{7,8}. Among the most concerning mechanisms are Extended Spectrum β -Lactamases (ESBLs) and resistance to amphenicols, due to their relevance for both human and animal health⁹. In Gram-negative bacteria, the *bla*CTX-M-15 and *flo*R are two of the most frequently reported antibiotic resistance genes (ARGs) within their respective classes, conferring resistance to β -lactam and amphenicol antibiotics, respectively¹⁰. *bla*CTX-M genes are represented by more than 50 allelic variants distributed over five major groups¹¹. Among these, *bla*CTX-M-15, a variant of the *bla*CTX-M-1 group, has the highest prevalence¹² (Figure S1A). Florfenicol-associated resistance genes, including *flo*R and *cfr*, have been widely reported, with *flo*R being the most prevalent^{13–15} (Figure S1B). While *bla*CTX-M variants have been primarily associated with bacterial human isolates^{12,16,17}, *flo*R has traditionally been linked to animal-derived bacterial isolates^{14,15}, as florfenicol is broadly used in livestock production. However, bacteria *flo*R-positive strains are increasingly detected in humans, particularly among individuals in close contact with poultry^{18,19}. Both ARGs have been detected in bacteria isolates from clinical^{16,19–21}, community-acquired^{18,22} animal^{14,15,23,24} and environmental samples including water^{25,26} and farms soil²⁶. The ARGs spread is enhanced by mobile genetic elements (MGEs), due to their ability to move within and between different host species²⁷. Among them, integrons are genetic elements that mobilize and express gene cassettes that confer resistance to antibiotics, disinfectants, heavy metals, and other pollutants²⁸. Although integrons are not mobile on their own, they are frequently integrated within transposons or carried on plasmids, facilitating their horizontal transfer²⁹. Class 1 integrons are the most prevalent in both clinical³⁰ and environmental^{29,31,32} contexts, particularly in *Enterobacteriaceae* clinical strains, such as *E. coli*³³ (Figure S1C). Its relative abundance has been proposed as

¹Biomolecules Laboratory, School of Biology, Faculty of Health Sciences, Universidad Peruana de Ciencias Aplicadas, Lima, Peru. ²Laboratorio de Microbiología Molecular, Laboratorios de Investigación y Desarrollo, Facultad de Ciencias e Ingeniería, Universidad Peruana Cayetano Heredia, Lima, Peru. ³School of Biosciences and Veterinary Medicine, University of Camerino, Camerino, Italy. ✉email: roberto.alcantara@upc.pe; pmilon@upc.pe

a marker of anthropogenic AMR pressure³⁴, since genomic analyses of cassette arrays frequently show co-occurrence with resistance to aminoglycoside, sulfonamide, tetracycline, β -lactams, and amphenicol^{35,36}. Due to its widespread distribution and frequent co-occurrence with multiple ARGs, detection of Class 1 integron could be used as a proxy to assess the ecological impact of human activity in AMR surveillance^{28,35}.

Currently, different methods for detecting antimicrobial resistance (AMR) are used, with the most common being antimicrobial susceptibility testing (AST) and molecular techniques such as PCR, qPCR, and DNA sequencing^{37,38}. While these methods are considered standards, there is a need of assays that combine the velocity provided by molecular methods with the low-costs of AST, and applicability in resource-limited or on-site settings. CRISPR/Cas technology has shown promising results for molecular detection approaches due to the high specificity, sensitivity, low costs, and speed of the assay³⁹. A molecular detection reaction based on CRISPR/Cas technology requires that the Cas enzyme: RNA complex scans the target sequence to identify the protospacer adjacent motif (PAM) region, denoted as TTTN for the Cas12a. Upon detecting the PAM, the complex opens the dsDNA template, allowing hybridization of the crRNA with the complementary region, ultimately rearranging the structure of Cas12a^{40,41}. This change triggers Cas12a to cut the template target site, known as cis-cutting activity. Subsequently, Cas12a engages in trans-cleaving activity, cutting ssDNA non-specifically⁴². When this action is linked to a fluorescence donor/quencher FRET pair placed into an oligonucleotide, it leads to an increase in fluorescence, which can be measured and recorded (Fig. 1A). Commonly nucleic acid detection by CRISPR/Cas12a requires a pre-amplification step to achieve a competitive analytical sensitivity⁴³. However, the pre-amplification is performed under some constraints. The primer set should amplify a DNA region that

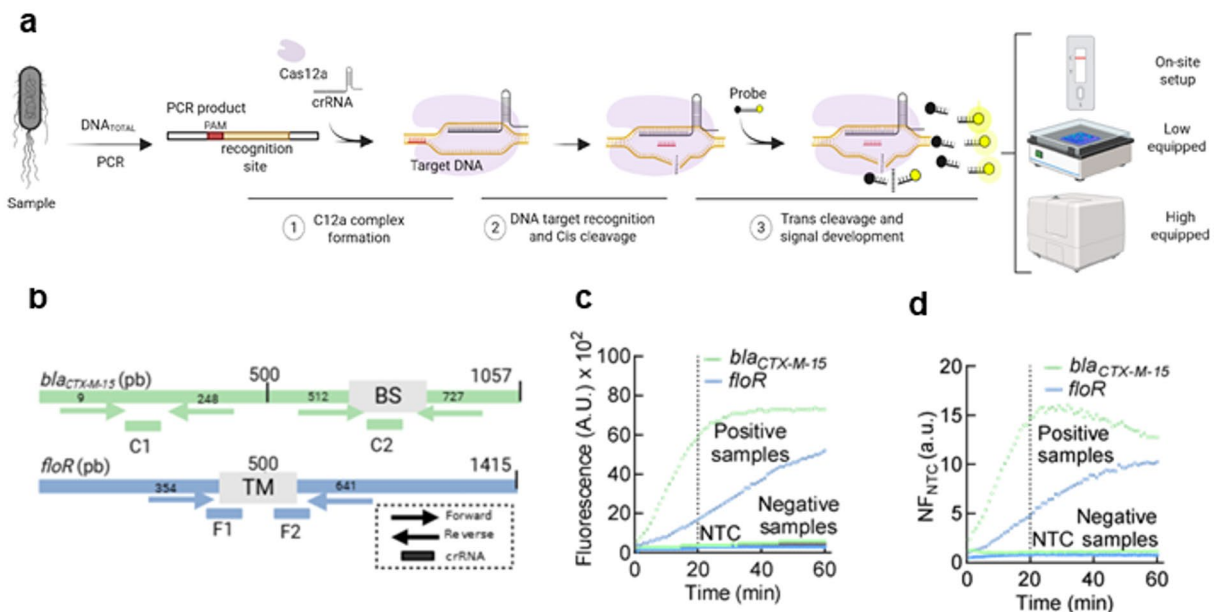


Fig. 1. Experimental setup for C12a development. **(A)** Scheme showing the C12a toolbox and the molecular mechanism of Cas12a-mediated detection, highlighting signal development, versatility, and diverse laboratory settings. A specific region containing the PAM and the recognition sites is amplified from DNA target. The amplified DNA is then recognized by the Cas: crRNA complex, which enables Cas cis-cleavage activity. Next, the activated nuclease complex performs trans cleavage on labeled probes, generating a detectable signal across diverse readouts formats. **(B)** Primers and crRNA target location on *bla*_{CTX-M-15} and *floR* gene targets. Primers are indicated by arrows. C1 and C2 indicate alternative complementarity sites for the crRNAs for *bla*_{CTX-M-15}. BS indicates the binding site of *bla*_{CTX-M-15} for beta-lactams. F1 and F2 indicate recognition sites for crRNAs against *floR*. TM indicates a transmembrane domain (151–202 aa). Primers amplify regions containing a PAM sequence and complementary to crRNAs targets. **(C)** Example of raw fluorescence readouts from CRISPR/Cas12a assays, showing a time-dependent increase of the signal. Positive and negative controls, alongside the Non-Template Control (NTC), are represented to illustrate the assay's ability to differentiate samples with or without ARGs. **(D)** Example of normalized fluorescence ratio NF_{NTC} (a.u.) over time. In **(C)** and **(D)**, the dotted line indicates the 20-minute detection point for fixed time analysis.

includes both a sequence complementary to the crRNA and a PAM site. Thus, differentially from PCR or qPCR, CRISPR/Cas12a adds a second specificity constrain provided by the crRNA complementarity to the target sequence.

Here, we present the C12a toolbox, a CRISPR-based set of molecular tools designed to detect genetic elements that confer antibiotic resistance or contribute to ARG propagation. The toolbox includes assays detecting *bla*CTX-M-15 (C12a^{bCTX}), *flo*R (C12a^{FLO}), and the *int*11 integrase gene (C12a^{INT}), selected for their relevance within the One Health framework. We describe the proof-of-concept, the biochemical and analytical validation of C12a as an adaptable platform optimized for high-, and low-equipped laboratories in addition to an on-site portable setting (Fig. 1C). Implementation of C12a nucleic acid-based technologies could effectively support fast, accurate, and sensitive detection, contributing to ARG surveillance efforts in a one health setup.

Results

C12a development

ARG detection sites were defined by comparing 61 *bla*CTX-M-15 and 46 *flo*R sequences from *E. coli* isolates available in GenBank (Supplementary Dataset 1 and Dataset 2, respectively). Based on consensus sequences two primer sets for *bla*CTX-M-15 and one for *flo*R were selected to amplify regions containing a PAM sequence for Cas12a (TTTN) (Fig. 1B, Figure S2, Table S2). Agarose gel electrophoresis confirmed amplification of *bla*CTX-M-15 (216 bp) and *flo*R (270 bp), with no bands in negative controls (Figure S3). Amplicons were sequenced to confirm the presence of the expected target DNA for each gene (Table S3). To optimize the crRNA/Cas12a reaction, two candidate crRNAs for each target gene were designed to contain a complementary sequence to the amplified fragments (Table S2). To determine sensitivity parameters, an initial test with increasing Mg²⁺ concentrations revealed an optimal value of 20 mM, which was used in all assays. Both *bla*CTX-M-15 and *flo*R amplicons were recognized by crRNA/Cas12a complex resulting in an increase in fluorescence signal (Figure S4). For *bla*CTX-M-15 target gene, primer set 2 combined with crRNA^{CTX-2}, showed greater fluorescence increase compared to crRNA^{CTX-1}. For *flo*R gene, crRNA^{FLO-1} outperformed crRNA^{FLO-2} (Figure S2). Thus, crRNA^{CTX-2} and crRNA^{FLO-1} were selected for further assays. Regardless of template concentration, crRNA^{CTX} consistently generated a fluorescence signal faster than the *flo*R crRNAs (Fig. 1B and Figure S2).

The results of this assay are reported as fluorescence ratio to the no-template control (NTC), indicated as NF_{NTC} (a.u.). To calculate NF_{NTC} , each raw fluorescence value was divided by the corresponding value from the NTC (Fig. 1C). For the *bla*CTX-M-15 gene, positive samples exhibited an NF_{NTC} of at least 14-fold, while negative samples displayed NF_{NTC} values near 1. Similarly, for the *flo*R gene, positive samples showed a 4-fold increase in NF_{NTC} compared to negative controls (Fig. 1C and Figure S2).

Based on performance, the final detection systems were defined. For *bla*CTX-M-15 detection, the C12a^{bCTX} system incorporates the primer set 2 and crRNA^{CTX-2} (Table S2). On the other hand, Cas12a^{FLO} detects *flo*R using the primer set 1 and the crRNA^{FLO-1} (Table S2).

C12a analytical sensitivity

Two key analytical parameters describe any given assay for analyte detection: the limit of blank (LoB; also referred to as the cut-off) and the limit of detection (LoD). The average NF_{NTC} values for ten negative samples using C12a^{bCTX} or C12a^{FLO} were 1.04 ± 0.02 and 0.94 ± 0.02 after 20 min of incubation (Figure S5). Here, we set the LoB as the average of true negative assays plus two standard deviations. Thus, the resulting LoB values were $1.08 NF_{NTC}$ (a.u.) for C12a^{bCTX} and $0.98 NF_{NTC}$ (a.u.) for C12a^{FLO}. Based on these values, we can state that 95.45% of the values below the determined LoB were likely to be classified as nonspecific background signals (i.e., signals in the absence of the analyte) (Figure S5).

To estimate the LoD for both detection systems, purified and quantified amplicons were tested at increasing concentrations (from 10^{-18} to 10^{-8} M, atto to nanomolar). Averaged NF_{NTC} (a.u.) values, measured at 10-minute intervals, were used to define the lowest detectable target concentration at the shortest reaction time. The LoD was calculated for each time interval, allowing the estimation of LoD as a function of reaction time (Fig. 2A). The time dependence indicates that after 21 min for C12a^{bCTX} and 17 min for C12a^{FLO}, the LoD reached half of its maximum value, suggesting that a 20-minute reaction time is a good compromise between assay speed and analytical sensitivity. The calculated LoD for C12a^{bCTX} and C12a^{FLO} at 20 min was 70 aM and 50 aM, respectively (Fig. 2B). Taking NF_{NTC} values at times shorter than 20 min (i.e. 10 min) would result in a tenfold loss in sensitivity (Fig. 2A).

We then assessed the analytical sensitivity of the CRISPR/Cas12a system in terms of the number of cells carrying the resistance genes (Fig. 2C). Bacterial cultures of true positive *E. coli* ranging from 3 to 3×10^6 CFU/mL were used (Figure S6). Non-linear fitting of the NF_{NTC} dependence on cell number (CFU) allowed the calculation of the LoD. C12a^{bCTX} reliably detected the *bla*CTX-M-15 gene at 77 CFU/mL, while C12a^{FLO} required 173 CFU/mL to detect *flo*R (Fig. 2C). The lowest target concentration that could be empirically detected for the two target genes was 10 to 100 times lower compared to gel electrophoresis analysis of PCR amplification (Fig. 2D, E, and Figure S7). Altogether, the detection and sensitivity performance of C12a^{bCTX} and C12a^{FLO} provide a solid foundation for testing the detection systems on a larger number of samples (see below).

ARG detection in *E. coli* isolates by C12a^{bCTX} and C12a^{FLO}

The presence of antibiotic resistance genes (ARGs) and the related phenotypic resistance in *E. coli* isolates was assessed by two distinct assays: (i) molecular detection using the C12a toolbox and (ii) antimicrobial susceptibility testing (AST) (Fig. 3). Two small independent sample sets were randomly selected from a collection of *E. coli* isolated from human sources in community settings (see Materials and Methods). Fifteen isolates were evaluated for the presence of *bla*CTX-M-15 and beta-lactam resistance, while seventeen were assessed for *flo*R and resistance to amphenicols. Phenotypic profiling was confirmed using the combined disk (CD) method for

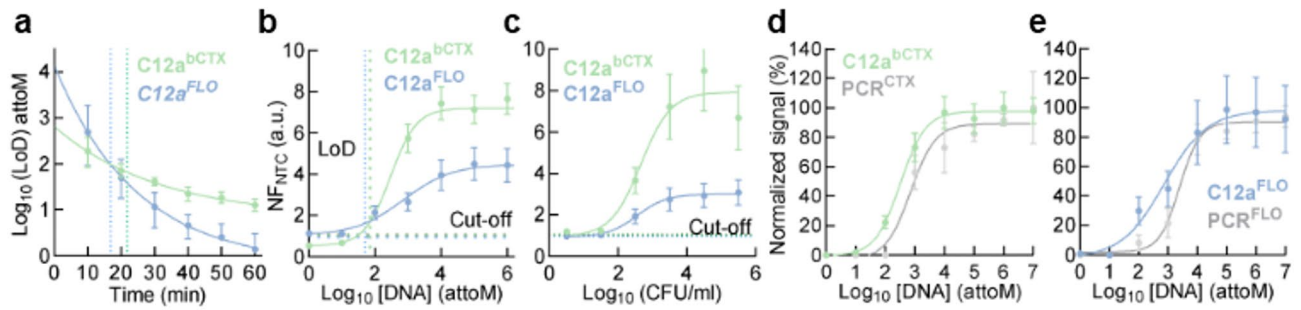


Fig. 2. C12a^{bCTX} and C12a^{FLO} Limit of Detection (LoD). **(A)** Time-resolved determination of LoD values for both ARGs Cas12a reactions, plotted on a logarithmic scale. The graph illustrates the LoD decrease for C12a^{bCTX} and C12a^{FLO} over incubation time, with dotted lines marking the time-point when the LoD reaches half of its maximum value. **(B)** Normalized fluorescence ratio as a function of target concentration for ARG detection assays. The vertical dotted lines represent the LoD value calculated at 20 min, while the horizontal dotted lines represent NF_{NTC} LoB (cutoff). **(C)** Normalized fluorescence ratio over bacterial cell concentration for both C12a assays. The dotted horizontal lines indicate average NF_{NTC} cut-off values of 1.08 and 0.98 for C12a^{bCTX} and C12a^{FLO}, respectively. **(D)** Normalized assay signals across target concentrations for C12a^{bCTX} detection compared to PCR-based detection evaluated by gel electrophoresis. The fluorescent ratio for the Cas12a reaction and electrophoresis gel band intensity, recorded as Area Under the Curve (AUC) values, are normalized as percentages to the highest value. **(E)** Same as (D), but for C12a^{FLO}. Error bars in all panels represent standard deviations from 3 replicates.

ESBL detection (Table S4) and broth microdilution to determine minimum inhibitory concentrations (MICs) for florfenicol (Table S5). The C12a^{bCTX} and C12a^{FLO} assays were then applied to their corresponding set to evaluate detection performance.

Out of 15 isolates, 7 were ESBL producers and found positive by C12a^{bCTX} for the presence of *bla*CTX-M-15 gene while 8 were susceptible to beta-lactams and found negative by the C12a toolbox (Fig. 3A). Similarly, C12a^{FLO} found the *floR* gene in 11 florfenicol resistant isolates, while susceptible isolates (6/17 isolates) turned out negatives by C12a (Fig. 3C) (Table S4-5). When assessing the performance of the C12a toolbox, NF_{NTC} values for ARG-positive samples ranged from 11 to 16 for C12a^{bCTX} and from 3 to 4.5 for C12a^{FLO} after 20 min of incubation, indicating the detection of the target genes. In contrast, ARG-negative samples showed no NF_{NTC} values higher than 1.0 with both C12a assays, indicating the absence of the target genes (Fig. 3A-C). Altogether, the noise to signal ratio, for positive samples, shown by the C12a toolbox was between 3- to 11- fold over the LoB. Full concordance was observed between the presence of resistance genes using the C12a toolbox and AST assays (Fig. 3B-D).

Detection of the *intI1* gene by C12a^{INT}

Using the C12a toolbox, we evaluated the detection of the *intI1* integrase gene, located in the 5' conserved region of the Class 1 integron. Previous studies suggested a correlation between *intI1* presence and MDR profiles^{35,36}. Here, we evaluated the detection of the *intI1* gene by designing a set of crRNAs (C12a^{INT}) and using a reported set of primers⁴⁴ (Table S2) to detect a 146 bp amplification product (Figure S8). Among the three candidate crRNAs, crRNA^{intI1c} showed better NF_{NTC} values at 20 min reaction time under standardized C12a reaction conditions (Fig. 4A). Using the C12a^{INT}, we detected the presence of the *intI1* gene in 17 out of 18 ARG-positive samples (Fig. 4C). Fluorescence ratios over the NTC control ranged between 3 and 10, showing greater dispersion if compared to the other C12a tools (Fig. 4B). Thus, the results could suggest that the presence of *intI1* is associated to *bla*CTX-M-15 or *floR*. However, several reports indicate that none of the evaluated ARG are usually located within the gene cassette for integron 1. To get further insights, we investigated the correlation by in silico analysis of sequencing data and characterize the integron structure and ARG content within cassette arrays (Fig. 4C). Data analysis of short reads using *bla*CTX-M-15 or *floR* positive *E. coli* isolates revealed that 11/18 carried a cassette array (61.1%), indicated by the presence of the attC recombination sites. The cassette array frequently contained genes conferring resistance to aminoglycosides (100%), trimethoprim (81.82%), phenicols (36.36%), lincosamide (27.27%) and sulfonamides (18.18%). Additionally, genes conferring tolerance to disinfectants such as *qacE* were observed in 5 isolates (45.45%) (Fig. 4C). The in-silico analysis revealed that transposons localized near Class 1 Integron were probably involved in the mechanism of acquisition and transfer of the observed cassette array. Consistent with previous reports, *bla*CTX-M-15 or *floR* genes were not found as part of the cassette arrays (Table S7). Our results suggest the potential of C12a^{INT} for Class 1 integron detection as proxy of multidrug resistance as previously described^{35,36}, however, direct ARG detection remains necessary for surveillance of specific genetic markers of antibiotic resistance.

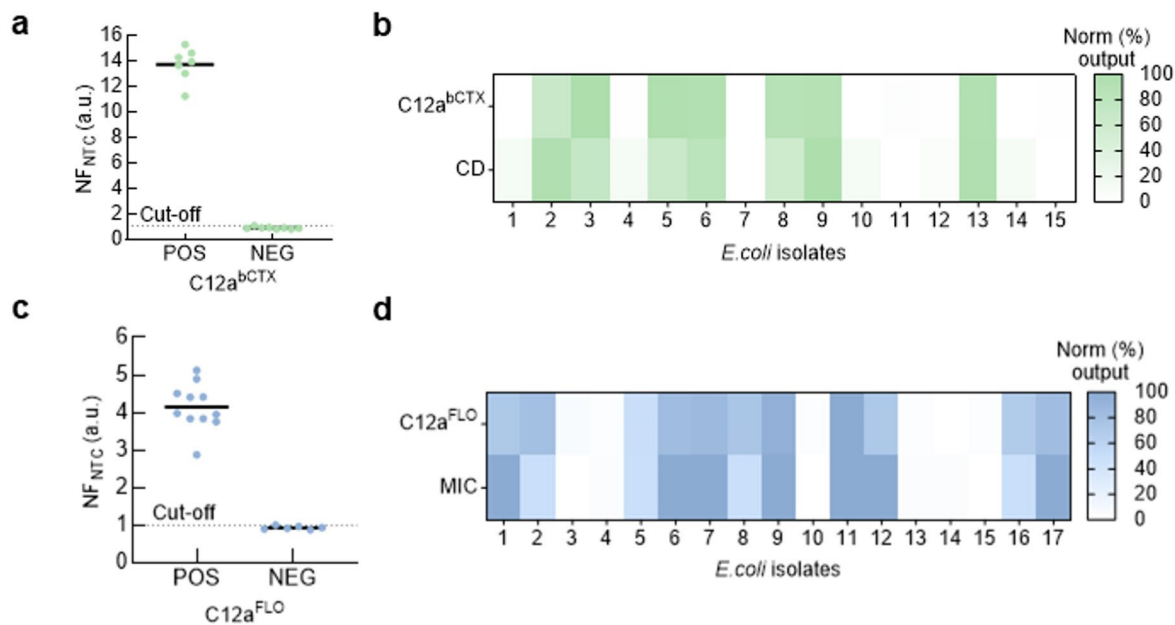


Fig. 3. C12a^{bCTX} and C12a^{FLO} comparison with AST methods. **(a)** Distribution of $bla_{CTX-M-15}$ detection in 15 isolates tested using the C12a^{bCTX} assay. The dotted line represents the measured LoB or cut-off. **(b)** Heat map comparing the C12a^{bCTX} assay (Top line of cells) with the disk diffusion test (CD) (Bottom line of cells). Cells in grades of green indicate a positive result in the respective assay. Both numerical readouts were normalized to the highest value within their respective data sets, and set to 100% (darker green). Lighter green colors represent lower fluorescent signals (Top line of cells) or CD values (bottom line of cells) (Table S4) **(c)** Distribution of $floR$ detection in 17 isolates tested using the C12a^{FLO} assay. The dotted line represents the measured LoB or cut-off. **(d)** Heat map comparing the C12a^{FLO} assay (Top line of cells) with MIC determination (Bottom line of cells). Cells in grades of blue indicate a positive result in the respective assay. Both numerical readouts were normalized to the highest value within their respective data sets, and set to 100% (darker blue). Lighter blue colors represent larger C12a^{FLO} (Top line of cells) or MIC (bottom line of cells) values (Table S5).

Efficient C12a-mediated ARGs detection in different laboratory setups

Differences in equipment availability may impact on the analytical performance of the C12a detection toolbox. To address this, we adapted our detection assays to three laboratory setups: (i) Low-equipped with minimal tools for qualitative readouts, such as a thermocycler and a transilluminator; (ii) portable setup using the Lateral Flow Assay (LFA) and transportable workstation (BentoLab[®]) suitable for on-site analysis, and (iii) High equipped with a multimode microplate reader for quantitative analysis, as used here for assay validation (Fig. 5).

Fourteen purified total fecal DNA available from the stool sample repository (BioProject number PRJNA821865) were analyzed with the C12a^{bCTX} and C12a^{FLO} assays across the three laboratory set-ups. For low equipped setup, direct visualization using a blue light transilluminator showed fluorescence in five out of 7 samples for $bla_{CTX-M-15}$. For $floR$, six out of seven samples resulted in fluorescence observation (Fig. 5A). The high-equipped setup showed that C12a^{bCTX} detected $bla_{CTX-M-15}$ in five samples, and two samples tested negative, respectively. All positive samples showed NF_{NTC} (a.u.) values exceeding 6 within 20 min. Similarly, for the C12a^{FLO}, NF_{NTC} (a.u.) values surpassing 3 were recorded at 20 min (Fig. 5B). For on-site setups, detection relied on LFA readouts instead of fluorescence detection. Here, a double-labeled probe with FITC and biotin is added in the CRISPR-Cas system allowing the appearance of two bands (the control line and test line) on the strip when an ARG is detected (Fig. 5C). No difference in detection performance was observed across all setups evaluated. Although the sample size was limited, these results suggest that the C12a toolbox demonstrates sufficient analytical sensitivity and robustness for ARG detection in total DNA samples across different laboratory setups.

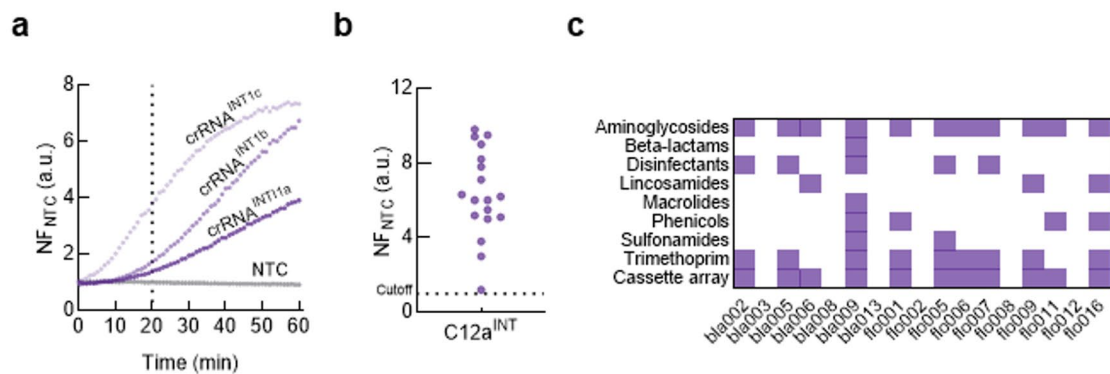


Fig. 4. C12a^{INT} detects the *int11* gene, as potential indicator of multidrug resistant *E. coli*. **(A)** Time-course of normalized fluorescence development for the C12a^{INT} assay with three crRNA designed to detect the *int11* gene. The vertical dotted line represents the incubation time used. **(B)** CRISPR-Cas detection of *int11* gene in 18 ARG-positive isolates tested using the C12a^{INT} assay. The dotted line represents the LoB at 1.0. **(C)** Heat map summarizing the antibiotic resistance genes related to different antibiotic families identified within the Class 1 integron cassette array of the ARG-positive *E. coli* isolates used in this study. ARGs were identified by bioinformatic analysis of genome sequencing data (BioProject number PRJNA821865).

Discussion

The global challenge of antimicrobial resistance (AMR) needs the development of new molecular detection strategies that are rapid, sensitive, cost-effective, and adaptable to diverse contexts, including clinical, veterinary, and environmental settings. Currently, antimicrobial susceptibility testing (AST) is widely used as routine assay in many health centers, along with molecular methods such as qPCR and DNA sequencing when they are affordable. While AST is highly specific and cost-effective, and molecular approaches are faster and highly sensitive, they remain limited by infrastructure, equipment, skilled personnel requirements, cost, or turnaround times^{37,38}. Therefore, there is a need for a compromise that combines the speed of ARG detection provided by molecular methods with AST costs. In this study, we presented the proof-of-concept of C12a for detecting key antibiotic resistance genes (ARGs) and associated elements. Although not yet validated for clinical or diagnostic use, the C12a toolbox demonstrates promising analytical features that could support future diagnostic development and surveillance efforts.

Molecular detection by C12a displays distinctive features: rapid (20 min detection, 100 min total analysis), high specificity due to the dual recognition steps mechanism that involves both primer selection and crRNA binding, competitive low limits of detection, and support for multiple readout formats, that make it suitable for various applications. CRISPR-Cas-based assays have demonstrated analytical performance comparable to well-established techniques, including qPCR, which remains the reference method in most molecular detection workflows⁴⁵. Previous studies showed complete concordance between CRISPR-Cas and qPCR results for the detection of genetic elements in pathogenic and virulence targets^{46–49}. While a direct comparison with qPCR was not conducted in this study, the C12a system showed strong signal-to-noise ratios, well-defined limits of blank (LoB), low limits of detection (LoD), and concordance with both AST and WGS analysis, reinforcing the reliability of the detection setup. Only a few CRISPR-based assays have been reported for ESBL detection, primarily targeting *blaSHV*, *blaOXA*, *blaNDM*, and most commonly *blaKPC*^{50–53}. No CRISPR-Cas12a based assays have been described for the *blaCTX* group. While reported detection limits vary by analyte, ranging from attomolar DNA fragments to 3×10^5 CFU/mL of whole bacteria^{54–58}. The turnaround times are largely consistent with our C12a-based method (70–120 min). Although some studies reported shorter times than those we observed, the differences likely result from the use of additive-supplemented buffers (e.g., HOLMES) or isothermal amplification methods (e.g., RPA or LAMP). For *floR*, we found no previously reported CRISPR-based assay. To the best of our knowledge, this is the first study to evaluate a CRISPR-based toolbox for detecting *blaCTX-M-15* and *floR* targets.

The targets selected for this study address both diagnostic relevance and ecological concern. Detection of *blaCTX-M-15* and *floR* genes are of increasing importance due to their widespread distribution across human, animal and environmental interfaces (Figure S1). Specifically, *blaCTX-M-15* has been traditionally associated with humans^{12,16} and *floR* with animals^{14,15}, however recent findings indicate that both genes are now being detected across diverse scenarios. Resistance gene *floR*, mainly linked to animal populations, has been recently identified in humans, highlighting its spread beyond conventional boundaries^{18,19,21}. These patterns of occurrence reflect the interconnected dynamics of AMR, where elements like Class 1 integrons, often inserted in transposons and plasmids, contribute to the spread of multidrug-resistant genes in various environments³⁶. Although our analysis revealed no integron association for *blaCTX-M-15* or *floR* in the tested isolates, the frequent co-occurrence of *int11* with other ARGs highlights its utility as a marker of anthropogenic AMR pressure^{28,31,35,36}. The development of a simplified detection system for ARGs is crucial for investigating AMR across a spectrum of contexts, from clinical settings to environmental and veterinary surveillance. Traditional assays often face

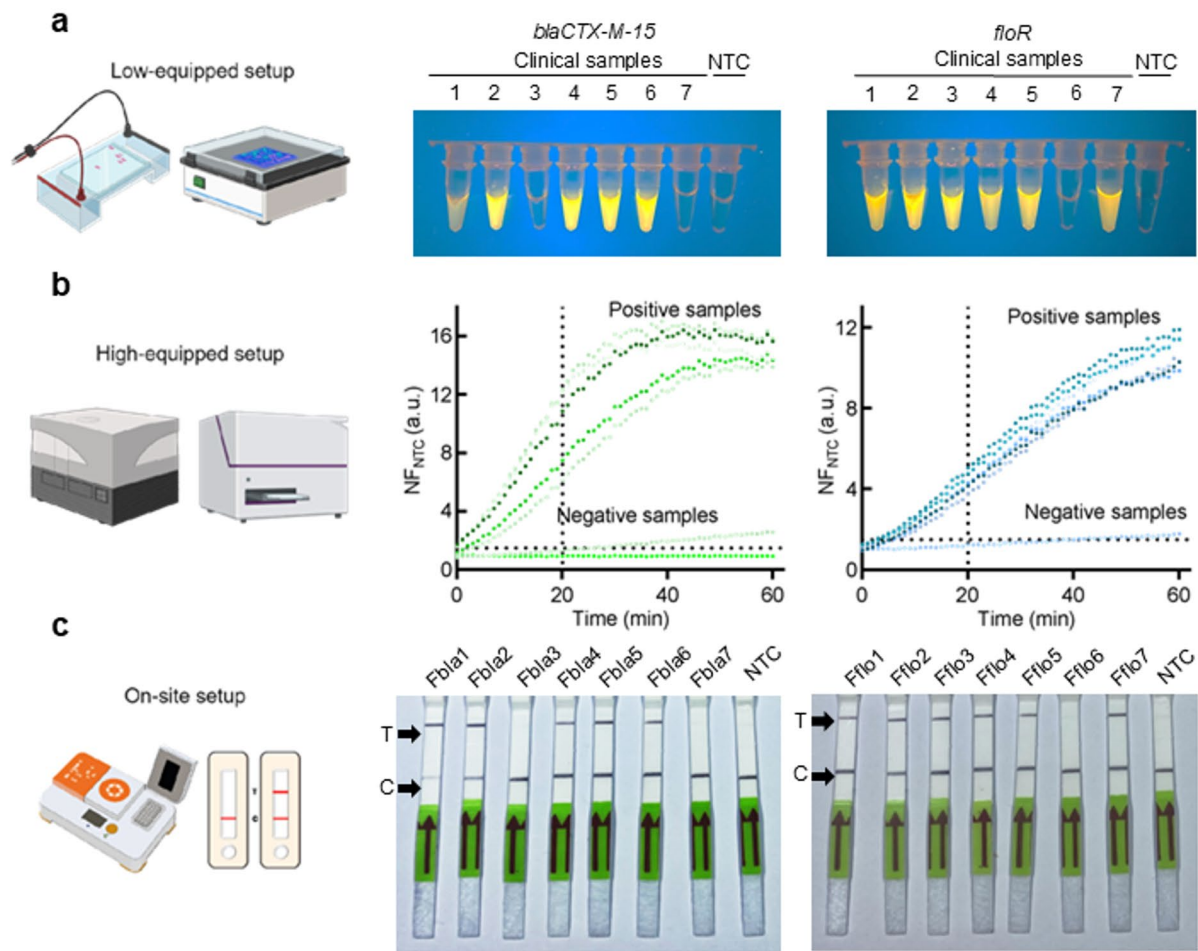


Fig. 5. C12a application across different laboratory setups. **(A)** *bla*CTX-M-15 and *flo*R detection in a low-equipped laboratory setup. Fluorescence was observed by direct visualization and photographed with a smartphone camera, default settings using a blue light transilluminator. **(B)** Similar to **(A)**, but for a high-equipped laboratory. NF_{NTC} (a.u.) values were measured over 60 min with a 20-minute detection cutoff. The horizontal dotted line represents an average NF_{NTC} cut-off value of 1.0. **(C)** Similar to **(A)**, but for an on-site setup. Detection by LFA strips readouts at 15 min incubation, where the T bands indicate the positivity of the test and C bands correspond to the control. NTC refers to non-template control.

limitations as previously described⁵⁹. Considering the substantial variations in laboratory resources across different institutions, having alternative readouts options with comparable performance is critical to keep AMR detection affordable, particularly in low-resource and field settings. The C12a toolbox addresses these limitations by being adaptable to laboratories with different levels of infrastructure and supporting multiple readouts formats. In our study, all enzymatic components were produced locally following an already published protocol⁶⁰ exemplify that the assay is accessible to even laboratories with minimal molecular biology equipment, accordingly to the advisable open-science strategy. C12a was successfully used with high-end equipment settings using fluorescence microplate readers, in low-tech settings using basic fluorescence visualization, and in portable formats using lateral flow assays (LFA). Performance was consistent across platforms, with only modest reductions in sensitivity observed in low-resource setups. These results suggest that the C12a system could support surveillance workflows in resource-limited environments. At this stage, the system has clear opportunities to broaden the target panel, compare its performance against qPCR, and evaluate it in clinical settings. As with other molecular assays, C12a detects resistance genes rather than phenotypic susceptibility, so further testing and optimization for varying sample types (e.g., water, soil), including other bacterial species are needed. Integration with mobile data platforms may also enhance usability for surveillance or epidemiological purposes.

In summary, this work presents a validated proof-of-concept for a CRISPR-Cas12a-based molecular detection system targeting relevant AMR genes along with MDR dissemination markers, that could potentially be used together as detection panel. Although not yet suitable for diagnostic implementation, the C12a toolbox demonstrates key features (velocity, sensitivity, specificity, and versatility) that are essential for future development of low-cost, field-adaptable AMR surveillance tools within a One Health framework and in low-resource settings.

Materials and methods

Biological samples

Two types of biological samples were used to evaluate the performance and adaptability of the C12a toolbox: (i) Total DNA extracted from *E. coli* isolates obtained from fecal samples and (ii) total DNA extracted directly from fecal material. All samples originated from a previously conducted community-based study involving children in Lima, Peru (NIH R01AI108695-01A1)⁶¹, which received ethical approval from the institutional review board at Universidad Peruana Cayetano Heredia (UPCH). All experiments were conducted in accord with the relevant guidelines and regulations, including identifying information. No demographic or identifying metadata from participants were accessed for this study.

A subset of positive and negative isolates for *bla*CTX-M-15 (bla001 – bla015, Table S4) and *floR* (flo001 – flo0017, Table S5) was randomly selected for the study. Only *E. coli* isolates positive for *bla*CTX-M-15 or *floR* were tested for the Class 1 integron detection. Total fecal DNA from a subset of samples (Fbla1 – Fbla7, and Fflo1 – Fflo7; Table S6) was used to evaluate the adaptability of the CRISPR assays across three laboratory configurations, including high-, low-, and portable-equipment settings.

Molecular stocks

A more detailed description of the molecular stocks design, synthesis or production (e.g., primers, crRNA and enzymes) is shared in the Supplemental material.

DNA purification: Total DNA was extracted from an *E. coli* culture grown to OD₆₀₀ = 0.7 using the Quick DNA Miniprep kit (Cat # D4069, Zymo Research) following the manufacturer's protocol. DNA was quantified using a NanoDrop spectrophotometer and stored at -20 °C. Amplicons were purified using the Oligo Clean Kit (Cat # D4060, Zymo Research). **Oligonucleotides synthesis:** Primers and crRNA DNA sequences were sourced from Macrogen Inc. (Seoul, South Korea). **crRNA synthesis:** crRNA was synthesized by in vitro transcription using the TranscriptAid T7 High Yield Transcription Kit (Cat#K0411, ThermoFisher Scientific) and purified with the RNA Clean & Concentrator Kit (Cat #11-353B, Zymo Research). **Enzymes:** Taq DNA polymerase and Cas12a proteins were sourced from locally expressed and purified stocks stored at -80 °C, as detailed in⁶⁰.

Antimicrobial susceptibility test

Combined disk test: The antibiotic susceptibility profile of 32 *E. coli* isolates was determined by the disk diffusion method, using *E. coli* ATCC 25,922 (Cat # 0335, Lab Elite) as the control strain. *E. coli* isolates from glycerol stocks were streaked on LB agar plates and incubated overnight at 37 °C. Isolated colonies were resuspended in 0.9% saline solution to a density of 0.5 McFarland and swabbed onto Mueller-Hinton agar plates (Cat # M173-500G, Himedia). Antibiotic disks, including cefotaxime (CTX) 30 µg (Cat # 9017, Liofilchem), and ceftazidime (CAZ) 30 µg (Cat # 9019, Liofilchem) were placed on the surface of the medium. After 18 h of incubation at 37°, inhibition zones were measured and interpreted following the CLSI guidelines. A confirmatory test for ESBL production, recommended by CLSI⁶², was performed using CTX 30 µg and CAZ 30 µg disks combined with clavulanic acid: CTX/AC 40 µg (Cat # 9182, Liofilchem), and CAZ/AC 40 µg (Cat # 9145, Liofilchem). Plates were incubated for 18 h at 37 °C, and ESBL producers were detected by measuring the difference in the inhibition halo of the antibiotic in the presence of clavulanic acid (> 5 mm). **Broth microdilution assay:** Florfenicol (Cat #F1427-500MG, Merck) was dissolved in dimethyl sulfoxide (DMSO) to a concentration of 100 mg/ml. Serial dilutions, ranging from 256 µg/ml to 0.125 µg/ml were prepared in a 96-well plate (Cat # 3596, ThermoFisher) using Mueller-Hinton Broth II (Cat # 610218, Liofilchem). Each well was inoculated with 1.5 × 10⁶ CFU/ml of cells. After 18 h of incubation at 37 °C, the MIC was determined according to CLSI guidelines⁶³. A MIC value of 32 µg/mL has been proposed as a tentative threshold to identify florfenicol-resistant *E. coli* isolates harboring the *floR* gene⁶⁴. However, it does not represent a formally established clinical breakpoint.

Bioinformatic analysis

To identify detection targets, all available *E. coli* resistance gene sequences for *bla*CTX-M-15 and *floR* in GenBank as of January 2022 were collected. Multiple alignment was performed, obtaining a consensus sequence of 1057 bp for *bla*CTX-M-15 and 1415 bp for *floR* (Supplementary Dataset 1 and Dataset 2, respectively). Primer sets were designed for the *bla*CTX-M-15¹⁶ and *floR*²¹ genes. For crRNA guide design and evaluation, CRISPRscan and Chop-Chop bioinformatics tools were used^{65,66}. DNA data analysis was downloaded from the BioProject web portal of the NCBI (<https://www.ncbi.nlm.nih.gov/bioproject/>) using accession code PRJNA821865. ARG presence was evaluated using the ResFinder platform (<http://genepi.food.dtu.dk/resfinder>) v4.6.0⁶⁷ with default parameters. Briefly, a minimum length of 60% and a threshold of 90% were set up for ARG and disinfectant-resistance gene identification. *E. coli* was defined as the species input. For the identification of the integrase-integron class 1, the VRprofile2 platform (<https://tool2-mml.sjtu.edu.cn/VRprofile/>)⁶⁸ with default parameters. Fluorescence data from the Synergy H1 plate reader were collected using Gen 5 software and exported to Excel. NF_{ntc} values were calculated during data processing and analysis as appropriate. All fluorescence data analysis and chart preparation were performed using GraphPad Prism version 10.0.0, www.graphpad.com.

C12a molecular assays

DNA amplification and analysis PCR conditions for amplifying the *bla*CTX-M-15 and *flo*R targets included an initial denaturation at 95 °C for 3 min, followed by 30 cycles of denaturation at 95° for 30 s, annealing at 59 °C for 30 s, extension at 72 °C for 30 s, and a final extension at 72 °C for 5 min. For the *int*I1 gene target, an annealing temperature of 60 °C was used. Amplification reactions (20 µL) contained 2 ng/µL Taq DNA polymerase, 0.2 µM primers, and 1 to 10 ng/µL of DNA in RPB1X buffer (Table S1). PCR products were visualized using 1.7% agarose gel electrophoresis (Cat # CSL-AG500, Cleaver Scientific) in 1X TBE buffer (Table S1) at 80 V for 1 h. Gels were stained with 6X Trick-Track – SYBR Gold (Cat #R1161, ThermoFisher) and visualized with a Gel Doc system (Bio-Rad) using the Sybergold option. A 100 bp molecular weight marker (Cat #SM0242, Thermo Scientific) was included. Band intensity was quantified as AUC using Gel Analyzer v23 (www.gelalyzer.com).

crRNA/Cas12a-mediated detection 150 nM crRNA was refolded (65 °C for 10 min, followed by 10 min at 25 °C) and assembled with 100 nM Cas12a, and 2 µM FAM probe (6-FAM/TTATT/3IABkFQ) in CRB1 buffer (Table S1) in the dark for 10 min. Unpurified PCR reactions containing amplicons (5 µL) were combined with 10 µL of the complex in CRB2 buffer (Table S1) to a final volume of 100 µL. Fluorescence was measured using a plate reader (Synergy H1, BioTek Instruments) with excitation at 491 nm and emission at 525 nm.

Lateral Flow Assay (LFA) CRISPR-Cas reaction was performed as described above using a biotin/fluorescein probe (6-FAM/TTATTATT/BIOTIN). The reaction buffer was supplemented with polyethylene glycol (Cat # 25322-68-3, Merck) to a final concentration of 5%. After 30 min of incubation, a LFA strip (Cat # 3822-9000, Milenia Biotec GmbH) was submerged in the reaction. The signal on the strips was detected after 5–10 min.

LoB and LoD determination Pure genomic DNA from ten susceptible *E. coli* isolates (true negative) were used to determine the LoB, using the formula $LoB = Avg_NF_{NTC} + 2 SD$ (where “Avg” is average NF_{ntc} values, and “SD” is standard deviation). The LoD was determined using both amplification products and bacterial cell counts for the *bla*CTX-M-15 and *flo*R targets. Amplicons were purified using the Oligo Clean Kit (Cat # D4060, Zymo Research) and quantified by absorbance at 260 nm. DNA concentrations ranged from 1 aM to 10 nM. The LoD was then estimated as the lowest DNA concentration above the $LoB + 2SD$ ⁶⁹. For the bacterial cell LoD determination, a curve was generated using a positive *E. coli* isolate culture. Starting from a cell density of 0.5 McFarland, and 7 ten-fold dilutions in duplicate. One set of dilutions was plated on LB agar plates for CFU counting, while the other set was analyzed directly with C12a.

Data availability

Sequence datasets generated and/or analyzed during the current study are available in the Mendeley Data repository, under the DOI: 10.17632/87n9k5zms4.1. Additionally, all generated data are included in this published article and its supplementary information files.

Received: 22 August 2025; Accepted: 24 February 2026

Published online: 01 March 2026

References

- Hutchings, M., Truman, A. & Wilkinson, B. Antibiotics: past, present and future. *Curr. Opin. Microbiol.* **51**, 72–80 (2019).
- Lipsitch, M. & Samore, M. H. Antimicrobial Use and Antimicrobial Resistance: A Population Perspective. *Emerg. Infect. Dis.* **8**, 347–354 (2002).
- Bungau, S., Tit, D. M., Behl, T., Aleya, L. & Zaha, D. C. Aspects of excessive antibiotic consumption and environmental influences correlated with the occurrence of resistance to antimicrobial agents. *Curr. Opin. Environ. Sci. Health.* **19**, 100224 (2021).
- Huijbers, P. M. C. et al. Role of the Environment in the Transmission of Antimicrobial Resistance to Humans: A Review. *Environ. Sci. Technol.* **49**, 11993–12004 (2015).
- Zhang, Z. et al. Assessment of global health risk of antibiotic resistance genes. *Nat. Commun.* **13**, 1553 (2022).
- von Wintersdorff, C. J. H. et al. Dissemination of Antimicrobial Resistance in Microbial Ecosystems through Horizontal Gene Transfer. *Front Microbiol* **7**, 173 (2016).
- Arnold, K. E. et al. The need for One Health systems-thinking approaches to understand multiscale dissemination of antimicrobial resistance. *Lancet Planet. Health.* **8**, e124–e133 (2024).
- Samreen, Ahmad, I., Malak, H. A. & Abulreesh, H. H. Environmental antimicrobial resistance and its drivers: a potential threat to public health. *J. Glob Antimicrob. Resist.* **27**, 101–111 (2021).
- Aslam, B. et al. Antibiotic Resistance: One Health One World Outlook. *Front Cell. Infect. Microbiol* **11**, 771510 (2021).
- Zhuang, M. et al. Distribution of antibiotic resistance genes in the environment. *Environmental Pollution* **285**, 117402 (2021).
- D’Andrea, M. M., Arena, F., Pallecchi, L. & Rossolini, G. M. CTX-M-type β-lactamases: A successful story of antibiotic resistance. *Int. J. Med. Microbiol.* vol. **303**, 305–317 (2013).
- Castanheira, M., Simner, P. J. & Bradford, P. A. Extended-spectrum β-lactamases: an update on their characteristics, epidemiology and detection. *JAC Antimicrob. Resist* **3**, 3 (2021).
- Escher, N. A., Muhummed, A. M., Hattendorf, J., Vonaesch, P. & Zinsstag, J. Systematic review and meta-analysis of integrated studies on antimicrobial resistance genes in Africa—A One Health perspective. *Tropical Med. Int. Health.* **26**, 1153–1163 (2021).
- Li, P. et al. Analysis of Resistance to Florfenicol and the Related Mechanism of Dissemination in Different Animal-Derived Bacteria. *Front Cell. Infect. Microbiol* **10**, 369 (2020).
- Ying, Y. et al. Florfenicol Resistance in *Enterobacteriaceae* and Whole-Genome Sequence Analysis of Florfenicol-Resistant *Leclercia adecarboxylata* Strain R25. *Int. J. Genomics* **2019**, 1–10 (2019).
- Ramadan, A. A., Abdelaziz, N. A., Amin, M. A. & Aziz, R. K. Novel blaCTX-M variants and genotype-phenotype correlations among clinical isolates of extended spectrum beta lactamase-producing *Escherichia coli*. *Sci Rep* **9**, 4224 (2019).
- Caballero, F. et al. Genomic diversity of uropathogenic *Escherichia coli* in clinical isolates from six latin american countries, 2018–2023. *Rev. Peru Med. Exp. Salud Publica.* **42**, 156–165 (2025).
- Murray, M. et al. Market Chickens as a Source of Antibiotic-Resistant *Escherichia coli* in a Peri-Urban Community in Lima, Peru. *Front Microbiol* **12**, 635871 (2021).

19. Lu, J. et al. Spread of the florfenicol resistance *floR* gene among clinical *Klebsiella pneumoniae* isolates in China. *Antimicrob. Resist. Infect. Control* **7**, 127 (2018).
20. Negeri, A. A. et al. Characterization of plasmids carrying *blaCTX-M* genes among extra-intestinal *Escherichia coli* clinical isolates in Ethiopia. *Sci. Rep.* **13**, 8595 (2023).
21. Qian, C. et al. Identification of *floR* Variants Associated With a Novel Tn4371-Like Integrative and Conjugative Element in Clinical *Pseudomonas aeruginosa* Isolates. *Front Cell. Infect. Microbiol* **11**, 685068 (2021).
22. Akenten, C. W. et al. Carriage of ESBL-producing *Klebsiella pneumoniae* and *Escherichia coli* among children in rural Ghana: a cross-sectional study. *Antimicrob Resist. Infect. Control* **12**, 1 (2023).
23. Gundran, R. S. et al. Prevalence and distribution of *blaCTX-M*, *blaSHV*, *blaTEM* genes in extended- spectrum β - lactamase-producing *E. coli* isolates from broiler farms in the Philippines. *BMC Vet. Res.* **15**, 227 (2019).
24. Higgins, O. et al. Portable Differential Detection of CTX-M ESBL Gene *blaCTX-M-1* and *blaCTX-M-15*, from *Escherichia coli* Isolates and Animal Fecal Samples Using Loop-Primer Endonuclease Cleavage Loop-Mediated Isothermal Amplification. *Microbiol. Spectr.* **11**, (2023).
25. Rangama, S. et al. Mechanisms Involved in the Active Secretion of CTX-M-15 β -Lactamase by Pathogenic *Escherichia coli* ST131. *Antimicrob Agents Chemother* **65**, 10 (2021).
26. Liao, C. Y. et al. Antimicrobial Resistance of *Escherichia coli* From Aquaculture Farms and Their Environment in Zhanjiang, China. *Front. Vet. Sci.* **8**, 1–12 (2021).
27. Tokuda, M. & Shintani, M. Microbial evolution through horizontal gene transfer by mobile genetic elements. *Microb Biotechnol* **17**, 1 (2024).
28. Gillings, M. R. et al. Using the class 1 integron-integrase gene as a proxy for anthropogenic pollution. *ISME J.* **9**, 1269–1279 (2015).
29. Zhang, S. et al. Dissemination of antibiotic resistance genes (ARGs) via integrons in *Escherichia coli*: A risk to human health. *Environ. Pollut.* **266**, 115260 (2020).
30. Bhat, B. A. et al. Integrons in the development of antimicrobial resistance: critical review and perspectives. *Front Microbiol* **14**, 1231938 (2023).
31. Corno, G. et al. Class 1 integron and related antimicrobial resistance gene dynamics along a complex freshwater system affected by different anthropogenic pressures. *Environ. Pollut.* **316**, 120601 (2023).
32. Stalder, T., Barraud, O., Casellas, M., Dagot, C. & Ploy, M. C. Integron involvement in environmental spread of antibiotic resistance. *Front Microbiol* **3**, 119 (2012).
33. Halaji, M. et al. The Global Prevalence of Class 1 Integron and Associated Antibiotic Resistance in *Escherichia coli* from Patients with Urinary Tract Infections, a Systematic Review and Meta-Analysis. *Microb. Drug Resist.* **26**, 1208–1218 (2020).
34. Stedtfield, R. D. et al. Isothermal assay targeting class 1 integrase gene for environmental surveillance of antibiotic resistance markers. *J. Environ. Manage.* **198**, 213–220 (2017).
35. Rao, S., Maddox, C. W., Hoiem-Dalen, P., Lanka, S. & Weigel, R. M. Diagnostic Accuracy of Class 1 Integron PCR Method in Detection of Antibiotic Resistance in *Salmonella* Isolates from Swine Production Systems. *J. Clin. Microbiol.* **46**, 916–920 (2008).
36. Solis, M. N. et al. Detecting Class 1 Integrons and Their Variable Regions in *Escherichia coli* Whole-Genome Sequences Reported from Andean Community Countries. *Antibiotics* **13**, 394 (2024).
37. Abramova, A., Berendonk, T. U. & Bengtsson-Palme, J. A global baseline for qPCR-determined antimicrobial resistance gene prevalence across environments. *Environ. Int.* **178**, 108084 (2023).
38. Abramova, A., Karkman, A. & Bengtsson-Palme, J. Metagenomic assemblies tend to break around antibiotic resistance genes. *BMC Genom.* **25**, 959 (2024).
39. Li, S. Y. et al. CRISPR-Cas12a-assisted nucleic acid detection. *Cell. Discov.* **4**, 20 (2018).
40. Stella, S., Alcón, P. & Montoya, G. Structure of the Cpf1 endonuclease R-loop complex after target DNA cleavage. *Nature* **546**, 559–563 (2017).
41. Stella, S. et al. Conformational Activation Promotes CRISPR-Cas12a Catalysis and Resetting of the Endonuclease Activity. *Cell* **175**, 1856–1871e21 (2018).
42. Broughton, J. P. et al. CRISPR–Cas12-based detection of SARS-CoV-2. *Nat. Biotechnol.* **38**, 870–874 (2020).
43. Zeng, D., Jiao, J. & Mo, T. Combination of nucleic acid amplification and CRISPR/Cas technology in pathogen detection. *Front. Microbiol.* **15**, 1355234 (2024).
44. Zhang, Y., Lu, J., Wu, J., Wang, J. & Luo, Y. Potential risks of microplastics combined with superbugs: Enrichment of antibiotic resistant bacteria on the surface of microplastics in mariculture system. *Ecotoxicol Environ. Saf* **187**, 109852 (2020).
45. Kaminski, M. M., Abudayyeh, O. O., Gootenberg, J. S., Zhang, F. & Collins, J. J. CRISPR-based diagnostics. *Nat. Biomed. Eng.* **5**, 643–656 (2021).
46. Wang, B. et al. Cas12aVDEt: A CRISPR/Cas12a-Based Platform for Rapid and Visual Nucleic Acid Detection. *Anal. Chem.* **91**, 12156–12161 (2019).
47. Wang, X. et al. Development and clinical application of a novel CRISPR-Cas12a based assay for the detection of African swine fever virus. *BMC Microbiol.* **20**, 282 (2020).
48. Wang, D. et al. A CRISPR/Cas12a-based DNzyme visualization system for rapid, non-electrically dependent detection of *Bacillus anthracis*. *Emerg. Microbes Infect.* **11**, 429–438 (2022).
49. van Dongen, J. E. & Segerink, L. I. Building the Future of Clinical Diagnostics: An Analysis of Potential Benefits and Current Barriers in CRISPR/Cas Diagnostics. *ACS Synth. Biol.* **14**, 323–331 (2025).
50. Curti, L. A. et al. CRISPR-based platform for carbapenemases and emerging viruses detection using Cas12a (Cpf1) effector nuclease. *Emerg. Microbes Infect.* **9**, 1140–1148 (2020).
51. Wang, S. et al. Detection of *Klebsiella pneumoniae* DNA and ESBL positive strains by PCR-based CRISPR-LbCas12a system. *Front. Microbiol.* **14**, 1128261 (2023).
52. Pablo-Marcos, D. et al. An accurate amplification-free CRISPR/Cas12a-based assay for GES β -lactamase detection. *Int. J. Antimicrob. Agents.* **66**, 107506 (2025).
53. Tyumentseva, M. et al. Ultrasensitive CRISPR/Cas12a-Based System for Detection of *BlaOXA-1* Gene in Antibiotic-Resistant Microorganisms. *Curr. Issues Mol. Biol.* **47**, 238 (2025).
54. Xu, H. et al. A New Method Based on LAMP-CRISPR-Cas12a-Lateral Flow Immunochromatographic Strip for Detection. *Infect. Drug Resist.* **15**, 685–696 (2022).
55. Tan, M. et al. Establishment of a platform based on dual RPA combined with CRISPR/Cas12a for the detection of *Klebsiella pneumoniae* and its KPC resistance gene. *Front Bioeng. Biotechnol* **12**, 1447963 (2024).
56. Shin, J., Kim, S. R., Xie, Z., Jin, Y. S. & Wang, Y. C. A CRISPR/Cas12a-Based System for Sensitive Detection of Antimicrobial-Resistant Genes in Carbapenem-Resistant Enterobacteriales. *Biosens. (Basel)*. **14**, 194 (2024).
57. Gao, Q. et al. Detection of KPC-Producing Carbapenem-Resistant *Klebsiella pneumoniae* Based on CRISPR Cas12a. *J. Microbiol. Biotechnol.* **35**, e2502042 (2025).
58. Demirayak, P. S. & Akay Sazaklioglu CRISPR for detection of drug resistance genes. *Clin. Chim. Acta.* **579**, 120626 (2026).
59. Kaprou, G. D., Bergšpica, I., Alexa, E. A., Alvarez-Ordóñez, A. & Prieto, M. Rapid Methods for Antimicrobial Resistance Diagnostics. *Antibiotics* **10**, 209 (2021).
60. Mendoza-Rojas, G. et al. A low-cost and open-source protocol to produce key enzymes for molecular detection assays. *STAR Protoc* **2**, 4 (2021).

61. Pajuelo, M. J. et al. Epidemiology of enterotoxigenic *Escherichia coli* and impact on the growth of children in the first two years of life in Lima, Peru. *Front Public Health* **12**, 1332319 (2024).
62. CLSI. Performance Standards for Antimicrobial Susceptibility Testing; Twenty-First Informational Supplement M100-S21. Wayne, PA, (2020).
63. CLSI. Methods for Dilution Antimicrobial Susceptibility Tests for Bacteria That Grow Aerobically M07-Ed12. Wayne, PA, (2024).
64. Singer, R. S. et al. Relationship between Phenotypic and Genotypic Florfenicol Resistance in *Escherichia coli*. *Antimicrob. Agents Chemother.* **48**, 4047–4049 (2004).
65. Labun, K. et al. CHOPCHOP v3: Expanding the CRISPR web toolbox beyond genome editing. *Nucleic Acids Res.* **47**, W171–W174 (2019).
66. Moreno-Mateos, M. A. et al. CRISPRscan: Designing highly efficient sgRNAs for CRISPR-Cas9 targeting in vivo. *Nat. Methods.* **12**, 982–988 (2015).
67. Bortolaia, V. et al. ResFinder 4.0 for predictions of phenotypes from genotypes. *J. Antimicrob. Chemother.* **75**, 3491–3500 (2020).
68. Wang, M. et al. VRprofile2: detection of antibiotic resistance-associated mobilome in bacterial pathogens. *Nucleic Acids Res.* **50**, W768–W773 (2022).
69. CLSI. *Evaluation of Detection Capability for Clinical Laboratory Measurement Procedures; Approved Guideline. CLSI Document EP17-A2* (Clinical and Laboratory Standards Institute, 2012).

Acknowledgements

We are very thankful to Dr. Maya Nadimpalli for promptly providing sequencing data of the *E. coli* isolate collection used in this study.

Author contributions

M.V.-R., R.A., M.P., and P.M. conceived the project. M.V.-R., R.A., and P.M. designed experiments. M.V.-R., R.A., and S.A. performed experiments. M.V.-R., R.A., and P.M. analyzed the data. M.V.-R., R.A., K.P., and P.M. elaborated figures and tables. R.S. and D.P. helped with data interpretation. M.V.-R., R.A., S.A., K.P., and P.M. wrote the manuscript with the input of D.P., R.S., and M.P.

Funding

This work was supported by the PROCENCIA program of CONCYTEC (Consejo Nacional de Ciencia, Tecnología e Innovación Tecnológica) with grant agreement PE501079419-2022 to PM. Seed funding was provided by the Universidad Peruana de Ciencias Aplicadas (C-004-2021-2) to RA. This work has received funding from the European Union's Horizon 2020 research and innovation program under the Marie Skłodowska-Curie grant agreement No 872869, supporting the international mobility of RA, SA, KP, PM, and RS. Additionally, this work received funding from the Fogarty International Center, National Institutes of Health (D43TW001140), to MP.

Declarations

Competing interests

The authors declare no competing interests.

Ethical approval

The *E. coli* isolates and DNA fecal samples used in this study were anonymous and derived from a biorepository of a longitudinal study approved by the ethics committee of Universidad Peruana de Cayetano Heredia (UPCH, SIDISI: 65178).

Additional information

Supplementary Information The online version contains supplementary material available at <https://doi.org/10.1038/s41598-026-42073-2>.

Correspondence and requests for materials should be addressed to R.A. or P.M.

Reprints and permissions information is available at www.nature.com/reprints.

Publisher's note Springer Nature remains neutral with regard to jurisdictional claims in published maps and institutional affiliations.

Open Access This article is licensed under a Creative Commons Attribution-NonCommercial-NoDerivatives 4.0 International License, which permits any non-commercial use, sharing, distribution and reproduction in any medium or format, as long as you give appropriate credit to the original author(s) and the source, provide a link to the Creative Commons licence, and indicate if you modified the licensed material. You do not have permission under this licence to share adapted material derived from this article or parts of it. The images or other third party material in this article are included in the article's Creative Commons licence, unless indicated otherwise in a credit line to the material. If material is not included in the article's Creative Commons licence and your intended use is not permitted by statutory regulation or exceeds the permitted use, you will need to obtain permission directly from the copyright holder. To view a copy of this licence, visit <http://creativecommons.org/licenses/by-nc-nd/4.0/>.

© The Author(s) 2026